Diagnostic Accuracy Study

Medicine®

OPEN

Diagnostic value of high b-value (2000 s/mm^2) DWI for thyroid micronodules

Qingjun Wang, MD[a], Yong Guo, MD[a,*], Jing Zhang, MD[a], Haoyong Ning, MD[b], Xiliang Zhang, MD[c], Yuanyuan Lu, MD[d], Qinglei Shi, MD[e]

Abstract

The aim of the study was to assess the diagnostic value of high b-value (2000 s/mm^2) diffusion-weighted imaging (DWI) in differentiating malignant from benign thyroid micronodules.

Consecutive patients with thyroid micronodules scheduled for Ultrasound (US)-guided fine-needle aspiration biopsy (FNAB) or surgery were underwent high b-value DWI with 3 b-values: 0, 800, and 2000 s/mm^2. Signal intensity ratios (SIRs) of thyroid micronodules to adjacent normal thyroid tissue on DWI were measured as SIR_{b0}, SIR_{b800} and SIR_{b2000}. Apparent diffusion coefficients (ADCs) according to the three different b-values were acquired as: $ADC_{b0–800}$, $ADC_{b0–2000}$ and $ADC_{b0–800–2000}$. The 6 diagnostic indicators were evaluated by receiver operating characteristic (ROC) and diagnostic ability was compared between the high b-value DWI and US.

Sixty-two malignant thyroid micronodules (48 patients, 13 men and 35 women, aged 44.8 ± 11.7 years) and 57 benign thyroid micronodules (40 patients, 6 men and 34 women, aged 49.6 ± 12.5 years) were enrolled into the final statistical analysis. Among the alone diagnostic indicators, SIR_{b2000} had the highest diagnostic ability in differentiating malignant from benign thyroid micronodules with area under curve (AUC) of 0.975, sensitivity of 90.32% and specificity of 96.49%. Compared to US, SIR_{b2000} had a significantly better diagnostic ability US for thyroid micronodules ($P < .001$) with dramatically raised positive predict value (96.6% vs 78.9%) and reduced false-positive rate (3.51% vs 26.32%).

High b-value (2000 s/mm^2) DWI can contribute to differentiating malignant from benign thyroid micronodules.

Abbreviations: 2D = two dimensional, ADC = apparent diffusion coefficient, AUC = area under curve, DW = diffusion-weighted, DWI = diffusion-weighted imaging, FNAB = fine-needle aspiration biopsy, IQ = image quality, MR = magnetic resonance, MRI = magnetic resonance imaging, MS-EPI = multi-shot echo-planar imaging, MTD = maximum transverse diameter, NTT = normal thyroid tissue, PTC = papillary thyroid carcinoma, PTMC = papillary thyroid microcarcinoma, RESOLVE = readout segmentation of long variable echo-trains, ROC = receiver operating characteristic, ROI = region of interest, SI = signal intensity, SIR = signal intensity ratio, T1WI = T1-weighted imaging, T2WI = T2-weighted imaging, TI-RADS = thyroid imaging reporting and data system, US = Ultrasound.

Keywords: diagnosis, differential, diffusion magnetic resonance imaging, high b-value, thyroid micronodules

1. Introduction

Thyroid nodules are detected in up to 50% to 60% of healthy subjects. According to World Health Organization,[1,2] when thyroid nodule is ≤ 10 mm in greatest diameter it is defined as micronodule, such as papillary thyroid microcarcinoma (PTMC). PTMC has recently become the most common pathological subtype in papillary thyroid carcinoma (PTC), which is the most common malignancy of the thyroid gland and accounts for 90% of all thyroid malignancies.[3] Although most PTMCs have benign behavior, little clinical significance, and do not affect patients' survival, aggressive behaviors including extrathyroidal extension, neck lymph node metastasis and distant metastasis can be found in some PTMCs patients.[4] Ultrasound (US) has been widely accepted as a standard imaging method for detection and diagnosis of thyroid nodules and US-guided fine-needle aspiration biopsy (FNAB) with cytological analysis is regarded as the most reliable diagnostic modality for evaluating thyroid nodules.[5] Being lack of ultrasonic malignant features, however, US is not an accurately diagnostic and surveillance method in PTMCs [6] and meanwhile, the American Thyroid Association guidelines do not recommend diagnostic US-guided FNAB for PTMCs given the unfavorable cost/benefit considerations.[4] Therefore, it is very important to find a reliable non-invasive imaging tool to diagnose and detect aggressive behavior of PTMCs and other malignant thyroid micronodules.

Previous studies have found that high b-value magnetic resonance (MR) diffusion-weighted imaging (DWI) with b-value greater than 1000 s/mm^2 can contribute to differentiation between benign and malignant lesions or between low- and high-grade tumors in prostate, brain, head and neck.[7–9] Furthermore, some studies have shown that high b-values in the range of 1500 to 2500

Editor: Neeraj Lalwani.

The authors have no conflicts of interest to disclose.

[a] Department of Radiology, [b] Department of Pathology, [c] Department of General Surgery, [d] Department of Ultrasound, Chinese Navy General Hospital of PLA, Fucheng Road, [e] Scientific Marketing, Siemens Healthcare Ltd., Zhonghuannan Road, Beijing, China.

[*] Correspondence: Yong Guo, Department of Radiology, Chinese Navy General Hospital of PLA, Fucheng Road, Beijing 100048, China (e-mail: guoyonghu27@163.com)

Medicine (2019) 98:10(e14298)

Received: 29 December 2017 / Received in final form: 18 October 2018 / Accepted: 7 January 2019

http://dx.doi.org/10.1097/MD.0000000000014298

s/mm^2 are optimal for magnetic resonance imaging (MRI) diagnosis and differential diagnosis in prostate cancer.[10,11] Therefore, the aim of this study was to evaluate the role of high b-value (2000 s/mm^2) DWI using multi-shot readout segmentation of long variable echo-trains (RESOLVE) in discriminating malignant from benign thyroid micronodules.

2. Materials and methods

2.1. Population inclusion criteria

From June 2015 to September 2017, patients planned for US-guided FNAB or thyroid surgery due to thyroid micronodules ($\leq$ 1.0 cm in US) were consecutively underwent a thyroid high b-value DWI. Within a week before the MRI examination, all patients had been performed thyroid US (Philips IU 22, L12–5 ultrasonic probe, 7.5–10.0 MHz) (by YY Lu who had 7 years' experience in conventional US and US-guided thyroid FNAB). This study was approved by our institutional review board. Written consent was obtained from all patients before the scans. There were two main reasons that these patients with micronodules were given the MRI examination before FNAB or thyroid surgery:

(1) micronodules themselves had been classified by US as more than category 4a (suspicious malignancy) based on Thyroid Imaging Reporting and Data System (TI-RADS) [12] and surgeons wished to verify the US diagnosis by another way; or
(2) although micronodules themselves were considered as category 2 or 3 (benignancy or most likely benignancy) by US on TI-RADS,[12] they were concurrent with other nodules ($>$ 1.0 cm) diagnosed as more than category 4a by US.

All patients underwent FNAB or thyroid surgery (by XL Zhang who had 15 years' experience in thyroid surgery) within 1 week after thyroid US and MRI examination.

2.2. Population exclusion criteria

Patients who had been performed thyroid FNAB or neck (including thyroid gland) radiotherapy, chemotherapy and surgery before MRI examination would be excluded from the study. Image quality (IQ) of each micronodule on (diffusion-weighted imaging) DW images with b-value of 2000 s/mm^2 was evaluated respectively according to 4-point scale depending on clarity of measured micronodules: 4 = excellent (no problems were noticed on images and micronodules were clearly shown), 3 = good (images suffered from only minor degradation and were suitable for the evaluation of micronodules), 2 = moderate (images were not good but usable for evaluation of micronodules), and 1 = poor (images precluded assessment of micronodules and thyroid gland was barely shown). Micronodules with IQ of 1 point or with unsuccessful location match between US and MRI would be excluded from the study.

2.3. Location of micronodules in US

For accurate match of each micronodule between US and MRI, location information of both anatomic site and distance data was acquired by US and MRI. The US doctor firstly determined the center of each micronodule and located the center into one of the following possible anatomic sites: the isthmus and quarters of the right or left lobe from upper to lower pole and then measured the distance data in transverse section according to the following methods: distances from the micronodule's center to thyroid nearest and farthest margins in US ($D_{US\_nearest}$ and $D_{US\_farthest}$).

2.4. MRI acquisition

All MRI examinations were performed with a 3.0T scanner (MAGNETOM Skyra, Siemens Healthcare, Erlangen, Germany) with a dedicated 8-channel bilateral surface coil for neck (Chenguang Medical Technologies CO., LTD, Shanghai, China) and a 4-channel soft surface coil for thoracic entrance (Siemens Healthcare Sector, Erlangen, Germany). The protocol was acquired in the following order: coronal T2-weighted imaging (T2WI), axial T1-weighted imaging (T1WI) and T2WI, and axial high b-value DWI using 3 b-values. The high b-value DWI was performed using multi-shot echo-planar imaging (MS-EPI) sequence with RESOLVE and Generalized Autocalibrating Partially Parallel Acquisitions techniques. Averages of the high b-value DWI were respectively 1 for b-value of 0 s/mm^2, 1 for b-value of 800 s/mm^2 and 4 for b-value of 2000 s/mm^2 and the second TE value (115 ms) belonged to a 2 dimensional (2D) navigator echo sequence which was used to eliminate signals with linear and non-linear phase errors, and robustly correct phase-induced motion artifacts. Three sets of DW images were automatically online acquired with the b-values of 0, 800, and 2000 s/mm^2. Meanwhile, by calculating apparent diffusion coefficient (ADC) in each pixel of each slice based on a mono-exponential model with the 3 sets of DW images,[13] 3 sets of ADC maps were reconstructed without noise filtering: $ADC_{b0–800}$, $ADC_{b0–2000}$ and $ADC_{b0–800–2000}$. The protocol parameters are shown in Table 1.

2.5. Match of micronodules between US and MRI

All images were transferred to a processing workstation (Syngo; Siemens) and were first qualitatively reviewed by a radiologist (J Zhang) who specialized in head and neck DWI and had more than 10 years' experience in MRI applications and was blinded to history, laboratory, US TI-RADS and pathological results of patients. Then the radiologist identified anatomic site of each micronodule's center in MRI according to the anatomic location information provided by the US doctor and measured the distance data on axial DW image (b-value of 0 s/mm^2) according to the following location method similar with US: distances from the nodule's center to thyroid nearest and farthest margins ($D_{MR\_nearest}$ and $D_{MR\_farthest}$). Distance data of each micronodule was further matched between US and MRI by comparing the deviation of location data: the absolute difference between $D_{US\_nearest}$ to $D_{MR\_nearest}$ ($D_{US\_MR\_nearest}$) and between $D_{US\_farthest}$ to $D_{MR\_farthest}$ ($D_{US\_MR\_farthest}$). Given potential measuring error between US and MRI, a successful match for each micronodule would be determined with the following two requirements:

(1) the micronodule's center was found at the same anatomic site in both US and MRI;
(2) absolute $D_{US\_MR\_nearest}$ was less than 3.0 mm and meanwhile absolute $D_{US\_MR\_farthest}$ was less than 5.0 mm.

Once a micronodule was successfully matched between US and MRI, the radiologist would assessed the IQ on DW images with b-value of 2000 s/mm^2 according to the scoring criteria.

2.6. Measurement of diagnostic indicators on MR images

For micronodules eligible for enrolling into the study, the slice with maximum transverse diameter (MTD) of each micronodule on DW images with b-value of 0 s/mm^2 was selected and a region of interest (ROI) was drawn to encompass whole solid component of micronodule on the slice. ROI was carefully

Table 1

Imaging protocol parameters of coronal T2WI, axial T1WI and T2WI, and axial high b-value DWI.

Parameters	Coronal T2WI	Axial T1WI	Axial T2WI	Axial high b-value DWI
Sequence	TSE	TSE	TSE	MS-EPI RESOLVE
Repetition time (ms)	3500	1490	3420	6200
Echo time (ms)	95	13	87	74/115
Fat suppression	Dixon	FS	FS	FS
Flip angle (°)	165	160	180	180
Section thickness (mm)	3	3	3	3
Section interval (mm)	0.3	0.3	0.3	0.3
Field of view (mm)	160	160	160	175
Matrix	224×320	256×320	256×320	174×174
Average	1	3	3	1, 1 and 4
Slices	24	24	24	24
Bandwidth (Hz/pixel)	300	250	260	685
Parallel acquisition factor	2	2	2	2
B-values (s/mm^2)	/	/	/	0, 800, and 2000
Readout segments	/	/	/	7
Acquisition time	2' 13"	2' 34"	2' 39"	14' 11"

T1WI = T1-weighted imaging, T2WI = T2-weighted imaging, DWI = diffusion-weighted imaging, FS = frequency-selective, MS-EPI = multi-shot echo-planar imaging, RESOLVE = readout segmentation of long variable echo-trains, TSE = turbo spin-echo.

drawn to avoid hemorrhage, necrosis, calcium, cystic changes, and vascular structures and copied to corresponding DW images with b-values of 800 and 2000 s/mm^2 respectively and then the 3 values of micronodule's signal intensity (SI_{nodule}) with b-values of 0, 800, and 2000 s/mm^2 were acquired: SI_{nodule_b0}, SI_{nodule_b800} and SI_{nodule_b2000}. Another ROI with an area of about 0.2 to 1.5 cm^2 (depending on the area of normal thyroid tissue) was place on normal thyroid tissue adjacent to the selected nodule in the same slice to acquire the SI of normal thyroid tissue with b-values of 0, 800, and 2000 s/mm^2: SI_{NTT_b0}, SI_{NTT_b800} and SI_{NTT_b2000}. If normal thyroid tissue could not be found in area adjacent to the selected nodule, ROI of SI_{NTT} would be placed in the contralateral normal thyroid tissue in the same slice. For the thyroid gland with Hashimoto thyroiditis, ROIs of SI_{NTT} would be placed in area where no nodules could be distinguishable with naked eyes. Ratio of SI_{nodule}/SI_{NTT} was respectively calculated on DW images with b-values of 0, 800, and 2000 s/mm^2: $SIR_{b0} = SI_{nodule\_b0}/SI_{NTT\_b0}$, $SIR_{b800} = SI_{nodule\_b800}/SI_{NTT\_b800}$ and $SIR_{b2000} = SI_{nodule\_b2000}/SI_{NTT\_b2000}$. MTD of each micronodule on DW images with b-value of 0 s/mm^2 was measured as DWI-MTD.

2.7. Pathology

If a micronodule was confirmed as a benignancy by FNAB, it would be followed up and its location information would be recorded in US. If a micronodule was confirmed as a malignancy by FNAB before surgery, total thyroidectomy would be given directly and the specimen of total thyroidectomy would be acquired for further paraffin section. If a micronodule was not given FNAB before surgery, lobectomy would be given first for intraoperative frozen section to determine the micronodule's nature. If the micronodule was diagnosed as a benignancy by intraoperative frozen section, total thyroidectomy would not be applied and the specimen of lobectomy would be acquired for further paraffin section. On the contrary, if the micronodule was diagnosed as a malignancy, total thyroidectomy would be further given and the specimen of total thyroidectomy would be acquired for further paraffin section.

For both intraoperative frozen section and paraffin section, an experienced pathologist (H Y Ning) would cut the thyroid specimen, where a micronodule had been successfully matched between US and MRI, into axial slices from upper to lower pole layer-by-layer every other 3.0 mm. Under the guidance of the US doctor and radiologist, the pathologist carefully identified and separated the micronodule for further histologic examination.

2.8. Statistical analysis

One-Sample Kolmogorov-Smirnov Test was used firstly for analysis of the normality of continuous variables. Quantitative variables with normal distribution were expressed as mean ± standard deviation. Quantitative variables without normal distribution were expressed as median (95% confidence interval ranges). Qualitative variables were expressed as percentages. Student unpaired *t* test (or Welch test for unequal variances) or χ^2 test was applied to compare the difference of continuous variables or qualitative variables of 2 groups. One-Way ANOVA test or nonparametric test (Kruskal-Wallis H) was applied to compare the difference of continuous variables or qualitative variables of 2 groups. The receiver operating characteristic (ROC) curve was used to obtain the diagnostic threshold, area under curve (AUC), sensitivity, specificity of these diagnostic indicators. The parameter with the best diagnostic performance among the 6 alone indicators would be combined with different kinds of indicators to explore the potentially better diagnostic ability of multi-parameters. The differences among the different diagnostic indicators in the high b-value DWI and the possible difference in diagnostic ability between the high b-value DWI and US were further compared by ROC comparison analysis. All statistical analysis were performed with MedCalc Software, version 11.4.2.0 (MedCal Software, Mariakerke, Belgium) and the level of statistical significance was determined by $P < .05$.

3. Results

3.1. Clinical-pathologic findings

According to the inclusion criteria, a total of 123 thyroid micronodules in 92 patients (23 men and 69 women, aged 47.0 ± 12.5 years old) underwent FANB or surgery and were confirmed as benign or malignant thyroid lesions by pathology. Four patients had both benign (n = 8) and malignant micronodules

(n = 6). There were 58 benign thyroid micronodules in 41 patients (7 men and 34 women): 35 simple nodular goiters, 10 nodular goiters complicated by adenomas, 4 nodular goiters complicated by Hashimoto thyroiditis, 2 nodular goiters complicated by Hashimoto thyroiditis and adenomas, 2 adenomas, 2 adenomas complicated by Hashimoto thyroiditis, 3 simple nodular Hashimoto thyroiditis. Four simple nodular goiters (in 4 patients) were confirmed by FANB and weren't performed thyroid surgery. There were 65 malignant micronodules in 51 patients (16 men and 35 women): 60 PTMCs (22 complicated with Hashimoto thyroiditis), 3 follicular thyroid carcinomas (2 complicated with Hashimoto thyroiditis) and 2 medullary thyroid carcinomas. Five micronodules of PTMC (in 5 patients) were confirmed directly by FANB and then were performed thyroid surgery. Two micronodules in 2 patients were given FANB, however, no meaningful tissues were found and then the 2 patient accepted thyroid surgery and consequently, the 2 micronodules were confirmed as PTMCs by postoperative pathology. The other micronodules were confirmed by postoperative pathology.

3.2. Match of micronodules between US and MRI

All these benign and malignant thyroid micronodules could be successfully matched between US and MRI. Of the 58 benign micronodules, 2 were located in the isthmus, 31 in the right lobe and 25 in the left lobe. Of the 31 benign micronodules in the right lobe, 4 were located in the first quarter, 10 in the second quarter, 9 in the third quarter and 8 in the fourth quarter. Of the 25 benign micronodules in the left lobe, 7 were located in the first quarter, 7 in the second quarter, 8 in the third quarter and 3 in the fourth quarter. Absolute $D_{US\_MR\_nearest}$ was 1.49 ± 0.63 mm and absolute $D_{US\_MR\_farthest}$ was 2.41 ± 0.89 mm. Of the 65 malignant micronodules, 6 were located in the isthmus, 22 in the right lobe and 37 in the left lobe. Of the 22 malignant micronodules in the right lobe, 4 were located in the first quarter, 5 in the second quarter, 7 in the third quarter and 6 in the fourth quarter. Of the 37 malignant micronodules in the left lobe, 11 were located in the first quarter, 8 in the second quarter, 11 in the third quarter and 7 in the fourth quarter. Absolute $D_{US\_MR\_nearest}$ was 1.39 ± 0.75 mm and absolute $D_{US\_MR\_farthest}$ was 2.61 ± 0.88 mm.

3.3. IQ of micronodules on high b-value DWI

The median (range) of IQ for the benign micronodules on high b-value DWI was 4 (1–4). Forty-three benign micronodules were scored as 4 points (43/58, 74.14%), 12 as 3 points (12/58, 20.69%), 2 as 2 points (2/58, 3.45%) and 1 as 1 point (1/58, 1.72%). The median (range) of IQ for the malignant micronodules on high b-value DWI was 4 (1–4). Forty-three malignant micronodules were scored as 4 points (43/65, 66.15%), 15 as 3 points (15/65, 23.08%), 4 as 2 points (4/65, 6.15%) and 3 as 1 points (3/65, 4.62%).

3.4. Summary of demographic features of study micronodules

One benign micronodule (a simple nodular goiter) in a patient was excluded from the study for the IQ with 1 point. Three malignant micronodules (3 PTMCs) in 3 patients were excluded from the study for the IQ with 1 point.

Therefore, 57 benign thyroid micronodules in 40 patients (6 men and 34 women, aged 49.6 ± 12.5 years old) were enrolled into the statistical analysis: 34 simple nodular goiters, 10 nodular goiters complicated by adenomas, 4 nodular goiters complicated by Hashimoto thyroiditis, 2 nodular goiters complicated by Hashimoto thyroiditis and adenomas, 2 adenomas, 2 adenomas complicated by Hashimoto thyroiditis, 3 simple nodular Hashimoto thyroiditis. There were 11 (11/57, 19.30%) benign micronodules related to Hashimoto thyroiditis (complicated by Hashimoto thyroiditis or nodular Hashimoto thyroiditis). The mean MTD of benign micronodules in US, DWI, and pathology was 7.60 ± 1.38 mm, 8.03 ± 1.98 mm and 7.70 ± 1.59 mm, respectively. There was no statistical difference in MTD of these micronodules between US, DWI and pathology ($\chi^2 = 2.395$, $P = .302$).

A total of 62 malignant thyroid micronodules in 48 patients (13 men and 35 women, aged 44.8 ± 11.7 years old) were enrolled into the statistical analysis: 57 PTCs (22 complicated with Hashimoto thyroiditis), 3 follicular thyroid carcinomas (2 complicated with Hashimoto thyroiditis) and 2 medullary thyroid carcinomas. There were 24 (24/62, 38.71%) malignant micronodules related to Hashimoto thyroiditis (complicated by Hashimoto thyroiditis). The mean MTD of malignant micronodules in US, DWI, and pathology was 7.56 ± 1.85 mm, 7.87 ± 2.59 mm and 7.60 ± 2.74 mm, respectively. There was no statistical difference in MTD of these micronodules between US, DWI and pathology ($\chi^2 = 0.278$, $P = .870$).

3.5. Comparison of diagnostic indicators of high b-value DWI between benign and malignant thyroid micronodules

Significant differences were found in all the 6 diagnostic indicators between the 2 groups (all $P < .05$, Table 2). Malignant micronodules showed a lower SIR_{b0} but higher SIR_{b800} and SIR_{b2000}, and lower ADCs (including $ADC_{b0–800}$, $ADC_{b0–2000}$, and $ADC_{b0–800–2000}$) than benign micronodules did (Table 2). Fig. 1 and Fig. 2 show the differences between benign and malignant thyroid micronodules in SIR and ADC.

3.6. ROC analysis of diagnostic indicators of high b-value DWI in differentiating malignant from benign thyroid micronodules

As can be seen in Table 3 and Fig. 3A, among the 6 diagnostic indicators of SIRs and ADCs the AUC of SIR_{b2000} were highest (0.975) with sensitivity of 90.32% and specificity of 96.49%. SIR_{b2000} combined with $ADC_{b0–800}$ had the highest AUC (0.987) with sensitivity of 93.55% and specificity of 100.0% among all these diagnostic indicators (alone or combined). Pair-wise comparison of the diagnostic performance between these alone or combined diagnostic indicators for distinguishing malignant thyroid micronodules are shown in Table 4. SIR_{b2000} exhibited

Table 2

Comparison of diagnostic indicators between benign and malignant thyroid micronodules.

Diagnostic indicators	Benign micronodules (n = 57)	Malignant micronodules (n = 62)	*P*
SIR_{b0}	2.34 ± 1.52	1.47 ± 0.51	$< .001^*$
SIR_{b800}	1.43 ± 0.68	2.09 ± 0.84	.001
SIR_{b2000}	0.86 ± 0.29	2.67 ± 1.44	$< .001^*$
ADC_{b0-800}	2.12 ± 0.51	1.30 ± 0.32	$< .001^*$
$ADC_{b0-2000}$	1.47 ± 0.33	0.92 ± 0.17	$< .001^*$
$ADC_{b0–800-2000}$	1.44 ± 0.32	0.89 ± 0.17	$< .001^*$

ADC = apparent diffusion coefficient (mm^2/s), SIR = signal intensity ratio.
* Welch-test assuming unequal variances.

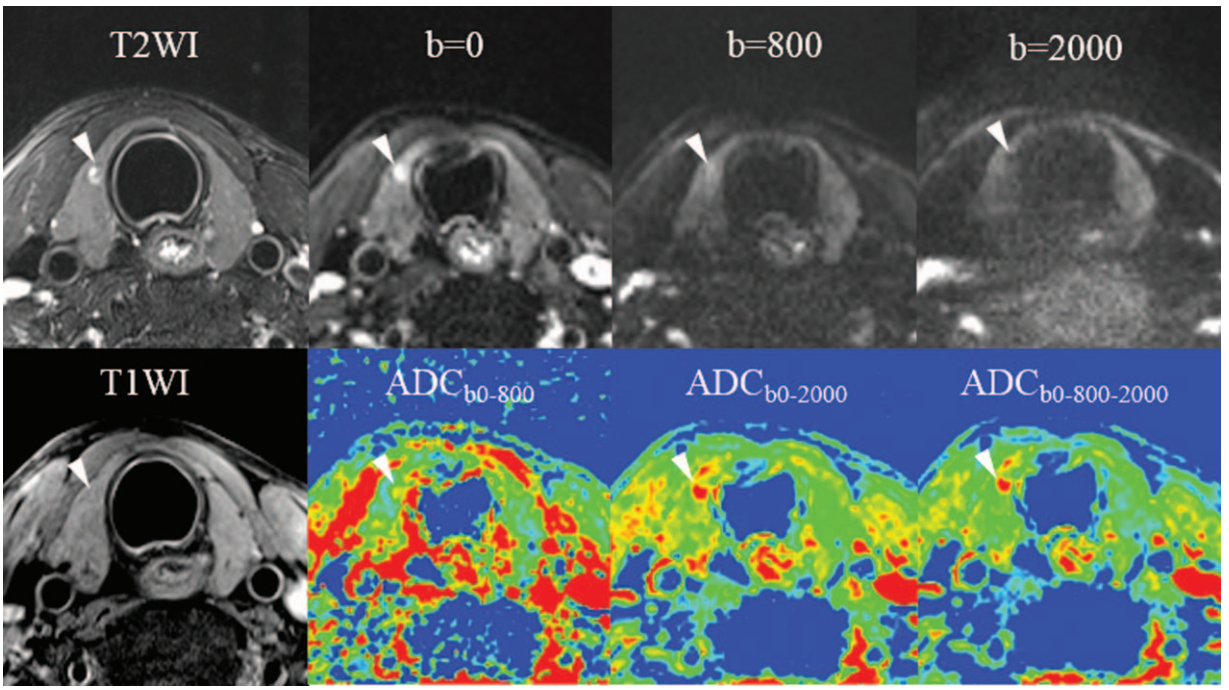

Figure 1. A micro-goiter in the right lobe (arrows-heads) in a 36-year-old man. SIR of the micro-goiter decreases with the b-values from 0 to 800 and 2000 s/mm^2. ADCs of the micro-goiter are higher than that of the normal thyroid tissue, especially on the ADC maps of $ADC_{b0–2000}$ and $ADC_{b0–800–2000}$. ADC = apparent diffusion coefficient, T1WI = T1-weighted imaging, T2WI = T2-weighted imaging.

significantly higher AUC than SIR_{b0} and SIR_{b800} did (both $P < .001$). There were significant differences between the 3 combined indicators and the other alone indicators (all $P < .05$), except for SIR_{b2000} (SIR_{b2000} vs SIR_{b2000} combined $ADC_{b0–800}$, SIR_{b2000} vs SIR_{b2000} combined $ADC_{b0–2000}$ and SIR_{b2000} vs SIR_{b2000} combined $ADC_{b0–800–2000}$, respectively; $P = .093$, .093 and .084; Fig. 3B). The 3 combined indicators did not show significant differences between each other (all $P > .05$).

3.7. Comparison of diagnostic ability between SIR_{b2000} and US in differentiating malignant from benign thyroid micronodules

SIR_{b2000} had significantly better diagnostic performance than US in discriminating malignant from benign thyroid micronodules (AUC: 0.975 vs 0.820; Youden index: 0.86 vs 0.64; $P < .001$; Tables 4 and 5 and Fig. 3C). Compared with US, SIR_{b2000} could

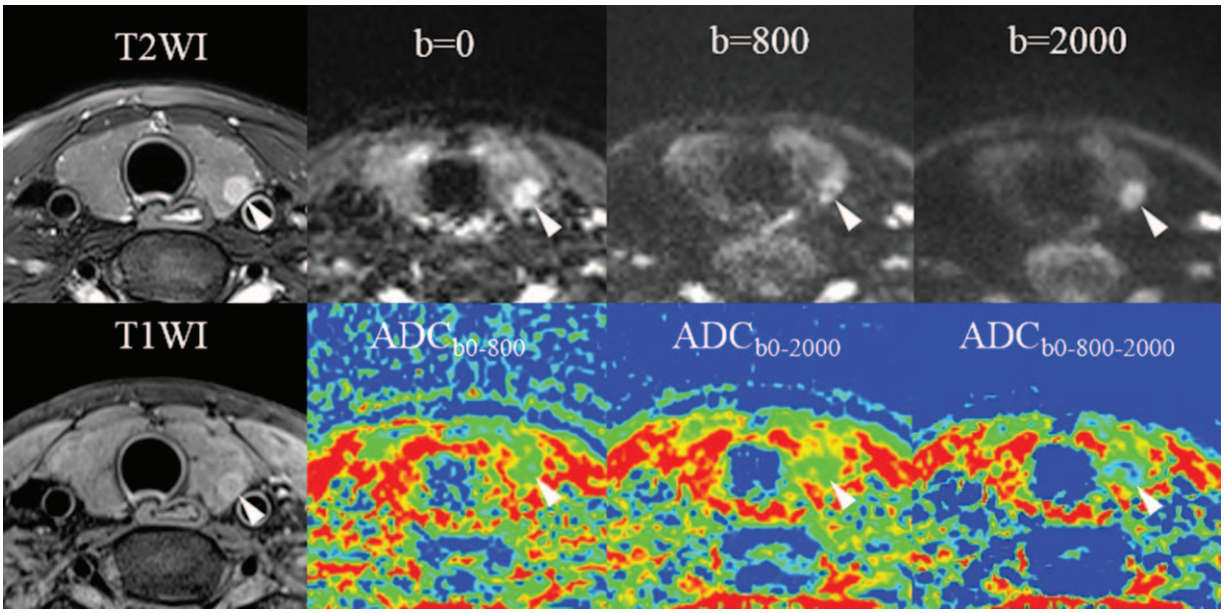

Figure 2. A papillary thyroid microcarcinoma (PTMC) in the left lobe (arrow-heads) in a 40-year-old woman. SIR of the lesion increases with the b-values from 0 to 800 and 2000 s/mm^2. ADCs of the lesion are markedly lower than that of the normal thyroid tissue, especially on the ADC maps of $ADC_{b0–2000}$ and $ADC_{b0–800–2000}$. ADC = apparent diffusion coefficient, T1WI = T1-weighted imaging, T2WI = T2-weighted imaging.

Table 3

ROC analysis of diagnostic indicators in differentiating malignant from benign micronodules.

Diagnostic indicators	Cutoff value	AUC	95% CI	Sensitivity (%)	95% CI	Specificity (%)	95% CI
SIR_{b0}	≤ 1.66	0.709	0.619–0.789	75.81	63.3–85.8	63.16	49.3–75.6
SIR_{b800}	> 1.63	0.748	0.660–0.823	70.97	58.1–81.8	71.93	58.5–83.0
SIR_{b2000}	> 1.46	0.975	0.929–0.995	90.32	80.1–96.4	96.49	87.9–99.6
$ADC_{b0–800}$	≤ 1.69	0.920	0.856–0.962	88.71	78.1–95.3	82.46	70.1–91.3
$ADC_{b0–2000}$	≤ 1.15	0.926	0.864–0.966	91.94	82.2–97.3	85.96	74.2–93.7
$ADC_{b0–800-2000}$	≤ 1.13	0.926	0.864–0.966	91.94	82.2–97.3	85.96	74.2–93.7
SIR_{b2000} + ADC_{b0-800}		0.987	0.947–0.999	93.55	84.3–98.2	100.0	93.7–100.0
SIR_{b2000} + $ADC_{b0-2000}$		0.985	0.943–0.998	93.55	84.3–98.2	96.49	87.9–99.6
SIR_{b2000} + $ADC_{b0–800–2000}$		0.986	0.945–0.999	95.16	86.5–99.0	96.49	87.9–99.6

ADC = apparent diffusion coefficient (mm^2/s), AUC = area under curve, CI = confidence interval, SIR = signal intensity ratio.

more effectively reduce the false malignant micronodules and contribute to an obviously higher positive predict value (96.6% vs 78.9%) and a markedly lower false-positive rate (3.51% vs 26.32%).

4. Discussion

Our study results revealed that malignant thyroid micronodules showed a lower SIR_{b0} but a higher SIR_{b2000} than benign thyroid micronodules did. ADCs of malignant thyroid micronodules were lower than that of benign thyroid micronodules with the same b-value. SIR_{b2000} had the best diagnostic performance in discriminating malignant from benign thyroid micronodules among all these alone diagnostic indicators. Although SIR_{b2000} combined different ADCs could improve the diagnostic performance, they did not show significant differences compared to SIR_{b2000}. If $SIR_{b2000} > 1.46$ was provided as a diagnostic cutoff value, the AUC, sensitivity and specificity were 0.975, 90.32%, and 96.49%, respectively. Compared with US, SIR_{b2000} could significantly increase positive predict value and decrease false-positive rate.

The reason that SIR_{b0} of malignant thyroid micronodules is lower than that of benign thyroid micronodules may be due to

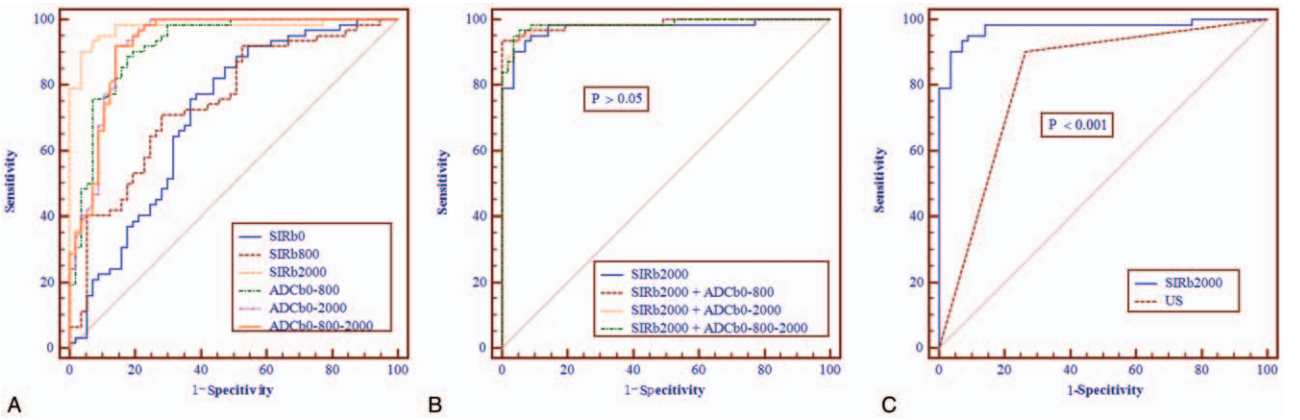

Figure 3. A, comparison of ROC curves between the alone diagnostic indicators in differentiating malignant from benign thyroid micronodules. B, comparison of ROC curves between SIR_{b2000} and combined indicators (SIR_{b2000} combined $ADC_{b0–800}$, SIR_{b2000} combined $ADC_{b0–2000}$ and SIR_{b2000} combined $ADC_{b0–800–2000}$). C, comparison of ROC curves between SIR_{b2000} and US. ADC = apparent diffusion coefficient, SIR = signal intensity ratio, US = Ultrasound.

Table 4

Comparison of the diagnostic ability between diagnostic indicators by pair-wise ROC analysis.

Diagnostic indicators *	SIR_{b0}	SIR_{b800}	SIR_{b2000}	$ADC_{b0–800}$	$ADC_{b0–2000}$	$ADC_{b0–800–2000}$	SIR_{b2000} + $ADC_{b0–800}$	SIR_{b2000} + $ADC_{b0–2000}$	SIR_{b2000} + $ADC_{b0–800–2000}$
SIR_{b0}	–	0.632	<0.001	< 0.001	< 0.001	< 0.001	< 0.001	< 0.001	< 0.001
SIR_{b800}	0.632	–	< 0.001	< 0.001	< 0.001	< 0.001	< 0.001	< 0.001	< 0.001
SIR_{b2000}	< 0.001	< 0.001	–	0.051	0.075	0.073	0.093	0.093	0.084
ADC_{b0-800}	< 0.001	< 0.001	0.051	–	0.760	0.773	0.007	0.011	0.010
$ADC_{b0-2000}$	< 0.001	< 0.001	0.075	0.760	–	1.000	0.015	0.017	0.016
$ADC_{b0–800-2000}$	< 0.001	< 0.001	0.073	0.773	1.000	–	0.014	0.016	0.015
SIR_{b2000} + ADC_{b0-800}	< 0.001	< 0.001	0.093	0.007	0.015	0.014	–	0.566	0.723
SIR_{b2000} + $ADC_{b0-2000}$	< 0.001	< 0.001	0.093	0.011	0.017	0.016	0.566	–	0.541
SIR_{b2000} + $ADC_{b0–800-2000}$	< 0.001	< 0.001	0.084	0.010	0.016	0.015	0.723	0.541	–

ADC = apparent diffusion coefficient (mm^2/s), ROC = receiver operating characteristic, SIR = signal intensity ratio.
* The results of the pairwise ROC comparison were *P* values.

Table 5

Comparison of the diagnostic ability between SIR_{b2000} and US in differentiating malignant from benign thyroid micronodules.

Imaging diagnosis *		Pathological results: Malignant micronodules (n = 62)	Pathological results: Benign micronodules (n = 57)	AUC	Sensitivity (%)	Specificity (%)	PPV (%)	NPV (%)	False-positive rate (%)	False-negative rate (%)	Youden index	*P*
SIR_{b2000}	Malignant micronodules	56	2	0.975	90.32	96.49	96.6	90.2	3.51	9.68	0.86	< .001
	Benign micronodules	6	55									
US	Malignant micronodules	56	15	0.820	90.32	73.68	78.9	87.5	26.32	9.68	0.64	
	Benign micronodules	6	42									

AUC = area under curve, NPV = negative predict value, PPV = positive predict value, SIR = signal intensity ratio, US = Ultrasound.

* According the ROC analysis, $SIR_{b2000} > 1.46$ was provided as a cutoff value for diagnosing malignant micronodules and $SIR_{b2000} \leq 1.46$ for diagnosing benign micronodules. Based on the previously published US criteria of TI-RADS, nodules with ≥ 4a were diagnosed as suspicious malignant micronodules and micronodules with 2 or 3 as benign lesions.

malignant micronodules' pathological features of fibrosis and microcalcification (especially in PTMCs).[14] It is well known that fibrosis or microcalcification usually present low signal intensity on T2W images. Therefore, it can be understood that malignant thyroid micronodules show lower SIR on DW images with b-value of 0 s/mm^2 than benign micronodules do, given the similar MRI characteristics between T2W images and DW images with b-value of 0 s/mm^2. This findings are similar to the results reported by Noda et al,[15] who observed that PTCs show lower SIR than benign thyroid nodules on T2W images. A previous study about breast DWI with multiple b-values by Han et al[16] demonstrated that sparse parenchymal cells, large intercellular spaces and relatively high diffusion of extracellular water molecules in benign breast lesions lead to gradually decreased SIR and on the contrary, compact parenchymal cells, small intercellular spaces and relatively low diffusion of extracellular water molecules in malignant breast lesions result in gradually increased SIR when b-values increased within a certain range (b-values from 0 to 1200 s/mm^2). Similar with the findings by Han et al[16], in our study the SIR of benign and malignant thyroid micronodules also showed a reversed change tendency with increasing b-values from 0 to 800 and 2000 s/mm^2, which lead to an obviously different SIR between the two groups when the b-value reached to 2000 s/mm^2. This significant SIR difference between benign and malignant thyroid micronodules on DW images with high b-value may help inexperienced radiologists to more easily detect and confidently diagnose malignant micronodules based on the high signal intensities and improve the diagnostic accuracy.

Previous review-studies[17,18] have demonstrated that ADC (b-values $\leq$ 1000 s/mm^2) of malignant thyroid nodules is significantly smaller than that of benign thyroid nodules, which help to discriminate malignant from benign thyroid nodules. In our study, ADCs with high b-values ($ADC_{b0–2000}$ and $ADC_{b0–800–2000}$) of malignant thyroid micronodules were also significantly smaller than that of benign thyroid micronodules. However, there were not significant differences in AUCs for diagnosing malignant thyroid micronodules between the three ADCs with various b-values combinations ($ADC_{b0–800}$, $ADC_{b0–2000}$ and $ADC_{b0–800–2000}$). When the three ADCs were combined with SIR_{b2000}, the 3 combined indicators exhibited significantly better diagnostic performance than all diagnostic indicators alone did except for SIR_{b2000}. This indicate 2 important points in differentiating malignant from benign thyroid micronodules in clinical scenario:

(1) compared to ADC with routine b-value, ADCs with high b-values may not obviously improve the diagnostic accuracy under the current analytical method;

(2) given that there was no significantly diagnostic difference between SIR_{b2000} and combined indicators (SIR_{b2000} combined different ADCs) and the feasibility of clinical application, SIR_{b2000} should be used alone as an important imaging parameter for thyroid micronodules.

Being limited by the poor quality image for thyroid micronodules on previous DWI protocol, few studies exclusively assess the value of DWI in detecting and diagnosing thyroid micronodules. Some studies on differentiation between benign and malignant thyroid nodules by DWI even excluded micronodules.[19–24] All these previous studies used a standard single shot echo planar imaging (SS-EPI) sequence for thyroid DWI. Due to the neck's complex structure with many boundaries between air and body surface, however, image quality of thyroid DWI is usually not satisfactory when the conventional SS-EPI is used. In this study, we applied thyroid DWI with multi-shot RESOLVE combined with a 2D-navigator–based reacquisition scheme, which can effectively reduce the concerned susceptibility artifacts, blurring from T2* signal decay and substantial distortion.[3,25] To confirm the superiority of multi-shot RESOLVE DWI over SS-EPI DWI in the neck area, Koyasu et al[26] compared image distortion and homogeneity of ADC maps between the two kinds of DWIs and they found that multi-shot RESOLVE DWI can provide higher-quality DW images with less distortion and more homogenous ADC maps than SS-EPI DWI. Considering the special position of thyroid gland, these properties are very important for high b-value DWI to clearly show thyroid micronodules. In our study, all the thyroid micronodules found by US could be detected by the high b-value DWI.

To compare the diagnostic ability between SIR_{b2000} in the high b-value DWI and US based on the standard TI-RADS criteria, some important diagnostic indexes were comparatively analyzed in differentiating malignant from benign thyroid micronodules. The diagnostic performance of SIR_{b2000} was significantly better than that of US, especially in the false-positive rate. Compared with US, SIR_{b2000} can markedly increases the positive predict value and decrease the false-positive rate. This demonstrates that versus US, high b-value DWI can preferably reduce the diagnostic mistakes that benign thyroid micronodules are misdiagnosed as malignant lesions and therefore can help to avoid unnecessary thyroid FNAB or surgery.

Our work has some limitations. Firstly, this study was a preliminary and non-registered single-center study and the patient samples were of insufficient size. A comprehensive and multicenter study based on registry and results database of a larger population is clearly warranted to derive more solid and convincing imaging indicators of thyroid micronodules. Secondly, only one high b-value (2000 s/mm^2) was selected in our study. The reason we chose the b-value of 2000 s/mm^2 is because

that previous studies have confirmed that b-values in the range of 1500 to 2500 s/mm^2 (but neither lower nor higher) are optimal for prostate cancer detection and diagnosis.[10,11,27] Considering that both of the thyroid gland and prostate gland are body's glandular organs, so we use the b-value of 2000 s/mm^2 for the high b-value DWI. However, a broader range of b-values for DWI on thyroid imaging should be investigated to determine the optimal b-value (s) of DWI in distinguishing malignant from benign thyroid micronodules.

5. Conclusions

Summarily, SIR_{b2000} of high b-value (2000 s/mm^2) DWI has the highest diagnostic ability and in discriminating malignant from benign thyroid micronodules among all the alone diagnostic indicators. Compared with US, SIR_{b2000} can obviously raise positive predict value and reduce false-positive rate.

Author contributions

Data curation: Xiliang Zhang, Qinglei Shi.
Methodology: Jing Zhang.
Software: Qinglei Shi.
Supervision: Haoyong Ning.
Validation: Yuanyuan Lu.
Writing – original draft: Qingjun Wang.
Writing – review & editing: Yong Guo.

References

[1] Sobin LH. Histological typing of thyroid tumours. Histopathology 1990;16:513.
[2] Dighe M, Luo S, Cuevas C, et al. Efficacy of thyroid ultrasound elastography in differential diagnosis of small thyroid nodules. Eur J Radiol 2013;82:e274–280.
[3] Schob S, Voigt P, Bure L, et al. Diffusion-weighted imaging using a readout-segmented, multishot EPI sequence at 3 T distinguishes between morphologically differentiated and undifferentiated subtypes of thyroid carcinoma-a preliminary study. Transl Oncol 2016;9:403–10.
[4] Haugen BR, Alexander EK, Bible KC, et al. 2015 American thyroid association management guidelines for adult patients with thyroid nodules and differentiated thyroid cancer: the american thyroid association guidelines task force on thyroid nodules and differentiated thyroid cancer. Thyroid 2016;26:1–33.
[5] Kim SK, Lee JH, Woo JW, et al. Prediction table and nomogram as tools for diagnosis of papillary thyroid carcinoma: combined analysis of ultrasonography, fine-needle aspiration biopsy, and BRAF V600E mutation. Medicine 2015;94:e760.
[6] Chen HY, Liu WY, Zhu H, et al. Diagnostic value of contrast-enhanced ultrasound in papillary thyroid microcarcinoma. Exp Ther Med 2016;11:1555–62.
[7] Kwak JT, Xu S, Wood BJ, et al. Automated prostate cancer detection using T2-weighted and high-b-value diffusion-weighted magnetic resonance imaging. Med Phys 2015;42:2368–78.
[8] Sui Y, Wang H, Liu G, et al. Differentiation of low- and high-grade pediatric brain tumors with high b-value diffusion-weighted MR imaging and a fractional order calculus model. Radiology 2015;277:489–96.
[9] Hwang I, Choi SH, Kim YJ, et al. Differentiation of recurrent tumor and posttreatment changes in head and neck squamous cell carcinoma: application of high b-value diffusion-weighted imaging. AJNR Am J Neuroradiol 2013;34:2343–8.
[10] Rosenkrantz AB, Parikh N, Kierans AS, et al. Prostate cancer detection using computed very high b-value diffusion-weighted imaging: how high should we go? Acad Radiol 2016;23:704–11.
[11] Agarwal HK, Mertan FV, Sankineni S, et al. Optimal high b-value for diffusion weighted MRI in diagnosing high risk prostate cancers in the peripheral zone. J Magn Reson Imaging 2017;45:125–31.
[12] Wang X, Wei X, Xu Y, et al. Ultrasonic characteristics of thyroid nodules and diagnostic value of Thyroid Imaging Reporting and Data System (TI-RADS) in the ultrosound evaluation of thyroid nodules. Zhonghua zhong liu za zhi [Chin J Oncol] 2015;37:138–42.
[13] Brown AM, Nagala S, McLean MA, et al. Multi-institutional validation of a novel textural analysis tool for preoperative stratification of suspected thyroid tumors on diffusion-weighted MRI. Magn Reson Med 2016;75:1708–16.
[14] Pusztaszeri MP, Sadow PM, Faquin WC. Images in endocrine pathology: psammomatoid calcifications in oncocytic neoplasms of the thyroid, a potential pitfall for papillary carcinoma. Endocr Pathol 2013;24:246–7.
[15] Noda Y, Kanematsu M, Goshima S, et al. MRI of the thyroid for differential diagnosis of benign thyroid nodules and papillary carcinomas. AJR Am J Roentgenol 2015;204:W332–335.
[16] Han X, Li J, Wang X. Comparison and optimization of 3.0 t breast images quality of diffusion-weighted imaging with multiple B-values. Acad Radiol 2016;7:
[17] Vermoolen MA, Kwee TC, Nievelstein RA. Apparent diffusion coefficient measurements in the differentiation between benign and malignant lesions: a systematic review. Insights Imaging 2012;3:395–409.
[18] Chen L, Xu J, Bao J, et al. Diffusion-weighted MRI in differentiating malignant from benign thyroid nodules: a meta-analysis. BMJ Open 2016;6:e008413.
[19] Shi HF, Feng Q, Qiang JW, et al. Utility of diffusion-weighted imaging in differentiating malignant from benign thyroid nodules with magnetic resonance imaging and pathologic correlation. J Comput Assist Tomogr 2013;37:505–10.
[20] Ilica AT, Artas H, Ayan A, et al. Initial experience of 3 tesla apparent diffusion coefficient values in differentiating benign and malignant thyroid nodules. J Magn Reson Imaging 2013;37:1077–82.
[21] Wu Y, Yue X, Shen W, et al. Diagnostic value of diffusion-weighted MR imaging in thyroid disease: application in differentiating benign from malignant disease. BMC Med Imaging 2013;13:23.
[22] Aydin H, Kizilgoz V, Tatar I, et al. The role of proton MR spectroscopy and apparent diffusion coefficient values in the diagnosis of malignant thyroid nodules: preliminary results. Clin Imaging 2012;36:323–33.
[23] Nakahira M, Saito N, Murata S, et al. Quantitative diffusion-weighted magnetic resonance imaging as a powerful adjunct to fine needle aspiration cytology for assessment of thyroid nodules. Am J Otolaryngol 2012;33:408–16.
[24] Bozgeyik Z, Coskun S, Dagli AF, et al. Diffusion-weighted MR imaging of thyroid nodules. Neuroradiology 2009;51:193–8.
[25] Porter DA, Heidemann RM. High resolution diffusion-weighted imaging using readout-segmented echo-planar imaging, parallel imaging and a two-dimensional navigator-based reacquisition. Magn Reson Med 2009;62:468–75.
[26] Koyasu S, Iima M, Umeoka S, et al. The clinical utility of reduced-distortion readout-segmented echo-planar imaging in the head and neck region: initial experience. Eur Radiol 2014;24:3088–96.
[27] Wetter A, Nensa F, Lipponer C, et al. High and ultra-high b-value diffusion-weighted imaging in prostate cancer: a quantitative analysis. Acta Radiol 2015;56:1009–15.